

# El Niño chaos: The role of noise and stochastic resonance on the ENSO cycle

Lewi Stone,<sup>1</sup> Peter I. Saperin,<sup>1</sup> Amit Huppert,<sup>1</sup> and Colin Price<sup>2</sup>

**Abstract.** An alternative approach for explaining aperiodicity and chaos in the El-Niño-Southern-Oscillation (ENSO) is proposed, which considers the ocean's equatorial wave dynamics as part of a nonlinear dynamical system driven by random environmental fluctuations. Noise excitation causes the model to jump chaotically between different interacting oscillations generated by the system's implied "Pacific ocean-atmosphere" cycle and the seasonal cycle. The injection of noise induces chaotic dynamics, triggering an El Niño whenever the model's thermocline depth exceeds a threshold level. A "stochastic resonance" arises – should noise intensity deviate substantially from optimal, the regular development and coherence of the ENSO cycle is impeded. The model's noise induced chaos provides an attractive explanation for the sporadic yet deterministic character of El Niño events.

## Introduction

El Niño, the anomalous warming of eastern equatorial waters of the Pacific, is a major climatic phenomenon that occurs sporadically every 3-7 years. The ENSO cycle's inherent irregularity is as much an undisputed fact as it is an enigma [Cane, *et al.*, in press]. One prominent school of thought argues that the majority of ENSO variability may be a form of correlated Gaussian noise and can be explained with a simple linear model driven by *external* stochastic forcing [Penland and Sardeshmukh, 1995]. This contrasts with a more recent competing view which asserts that the irregular ENSO oscillation is possibly a manifestation of low-dimensional deterministic chaos arising from the *internal* nonlinear interaction of the Pacific ocean-atmosphere system; if so it would account for the erratic character of the ENSO phenomenon as well as its more regular deterministic features such as El Niño's locking to the seasonal cycle (El Niño usually peaks close to December) [Munnich, *et al.*, 1991; Tziperman, *et al.*, 1994]. Here we borrow from both of these perspectives by examining the effects of noise forcing on a nonlinear deterministic ENSO model. We show that noise may play a crucial role in controlling the ocean-atmosphere dynamics and possibly result in chaotic ENSO oscillations.

The model is couched in terms of the ENSO "delayed

oscillator" paradigm [Graham and White, 1988; Munnich, *et al.*, 1991]. In brief, wave dynamics lead to oscillations between cold and warm ENSO phases as follows. Easterly winds lead to upwelling (cold sea surface temperatures (SST)) and the establishment of a shallow thermocline in the eastern Pacific, in contrast to a deep thermocline in the western Pacific (warm SST). As the zonal easterly winds drop in intensity, an equatorial Kelvin wave propagates from the central Pacific to the South American coast, deepening the thermocline as it travels eastward, thereby warming the SST – this is the initiation of the warm phase of the El Niño. A key component of the cycle is the propagation of Rossby waves which travel westwards from the central Pacific. Upon arriving at the western boundary these waves are reflected back eastward as equatorial Kelvin waves, eventually terminating El Niño, and possibly harbouring in the cold ENSO phase – La Niña. The ENSO cycle repeats with intensity, frequency and regularity that is dependent on the coupling of the ocean-atmosphere system

## The model

We make use of an existing heuristic model of these equatorial wave dynamics in which the key variable  $h(t)$  represents the deviation of the eastern thermocline depth from its average seasonal depth values, and which satisfies the delay-differential equation [Tziperman, *et al.*, 1994]:

$$\frac{dh}{dt} = aA[h(t - \tau_1)] - bA[h(t - \tau_2)] + c \cos(2\pi f_0 t) + D\xi(t), \quad (1)$$

$A(h)$  is a nonlinear function relating wind stress to SST and thermocline depth, with a form that qualitatively resembles the gradient of the vertical temperature profile of the ocean (full details and definition given in [Munnich, *et al.*, 1991]). The model's behaviour is controlled via the nonlinearity of  $A(h)$  by the parameter  $\kappa$  which governs the coupling between ocean and atmosphere. The first term in Eq.1 represents a Kelvin wave travelling to the eastern boundary in  $\tau_1 = 1.15$  months, while the second term represents the associated delayed Rossby wave travelling first to the western boundary where it is reflected as a Kelvin wave to arrive at the eastern boundary in a total time  $\tau_2 = 5\tau_1$  [Tziperman, *et al.*, 1994]. The periodic cosine term represents the effects of the seasonal cycle, which is modelled as an external forcing. Lastly,  $\xi(t)$  is Gaussian distributed white noise with  $\langle \xi \rangle = 0$ ,  $\text{Var}(\xi) = 1$ . The parameter  $D$  quantifies the intensity of the noise injected daily into the system relative to the amplitude  $c$  of the seasonal cycle. Model parameters in Eq.1 were taken as in [Tziperman, *et al.*, 1994] and [Stone & Saperin *ms.*] with  $a = 1/180$ ,  $b = 1/120$  and  $c = 0.9/138$ . We worked with both the raw time-series  $h(t)$ , and its smoothed counterpart obtained by passing  $h(t)$

<sup>1</sup>The Porter Super-Center for Ecological and Environmental Studies, Tel Aviv University, Israel.

<sup>2</sup>Department of Geophysics and Planetary Sciences, Tel Aviv University, Israel.

through a 12-month moving average filter, to suppress intra-annual variability [Tziperman, *et al.*, 1994, 1995].

In the absence of noise ( $D = 0$ ), the model is known to follow the quasiperiodicity route to chaos that arises from the nonlinear interaction of two frequencies – the annual seasonal cycle of frequency  $f_0$  and the model's intrinsic 3–4 year ENSO cycle of frequency  $f_1$  [Tziperman, *et al.*, 1994]. The bifurcation diagram [Stone & Saparin *ms.*], which summarises the dynamics of Eq.1 for different values of the control parameter  $\kappa$ , was obtained after strobing the solution of Eq.1 every 12 months. Under conditions of relatively weak nonlinearity ( $0 < \kappa < 1.231$ ), only the periodic annual cycle  $f_0$  is apparent and represented by a single point solution. Increasing  $\kappa$  just beyond  $\kappa = 1.231$  leads to bifurcation and the birth of a torus (in appropriate phase space), with quasiperiodic dynamics resulting from the interaction of two incommensurate frequencies  $f_0$  and  $f_1$ . (Quasiperiodic motion is simply the interaction of two periodic cycles whose frequencies are incommensurate i.e.,  $f_1/f_0$  is irrational.) For larger values of  $\kappa$ , regions of frequency-locking and chaos occur. When chaotic, the two oscillations,  $f_0$  and  $f_1$  compete simultaneously, and the dynamics of the trajectory jumps erratically between the two frequencies and their harmonics. This mechanism has been suggested as the likely cause of El Niño's irregularity [Tziperman, *et al.*, 1994, 1995; Chang, *et al.*, 1995].

### Noise induced effects and Stochastic Resonance

Here we report another important route to chaos and its attendant irregular oscillations. When Eq.1 is parametrised for strictly periodic or quasiperiodic oscillations, it is possible to induce chaotic dynamics simply by perturbing the model with noise ( $D > 0$ ), i.e., without any need for boosting the nonlinear ocean-atmosphere coupling  $\kappa$ . As shown in Fig.1, when the unperturbed model is parametrised for regular quasiperiodic dynamics ( $D = 0$ ,  $\kappa = 1.4$ , Fig.1a), stochastic forcing is all that is required to induce aperiodic chaotic oscillations closely locked to the seasonal cycle (Fig. 1b,  $D = 0.15$ ). Chaotic dynamics were diagnosed from a study of the time-series' largest Lyapunov exponent which was found positive, and by noting characteristic signs of torus destruction in the power spectrum. The spontaneous generation of chaos in systems with parameters tailored for periodic or quasiperiodic dynamics, may arise when perturbations promote random jumping between coexisting regular and chaotic attractors (of different stabilities), leaving the impression of "chaotic stochasticity."

A particular feature of the noise-induced chaos is the distinctive intermittency or "regime like behaviour" [Cane, *et al.*, in press] in the time series which arise when the trajectory hops erratically between the longer ( $\geq 3$  year) chaotic oscillation, and the annual saddle cycle ( $f_0$ ) that sporadically entrains the system (Fig.1b). Perhaps most importantly, the regime like behaviour has much in common with the dynamics observed in more complex ENSO models, where regions of quiescence are often followed by bursts of activity (Fig.1c). This behaviour has proved to be the major distinguishing feature of nonlinearity in the ENSO system [Cane, *et al.*, in press]; it is highly atypical for linear Gaussian processes. As Fig.1c displays, runs of the more sophisticated Cane-Zebiak (CZ) model [Zebiak

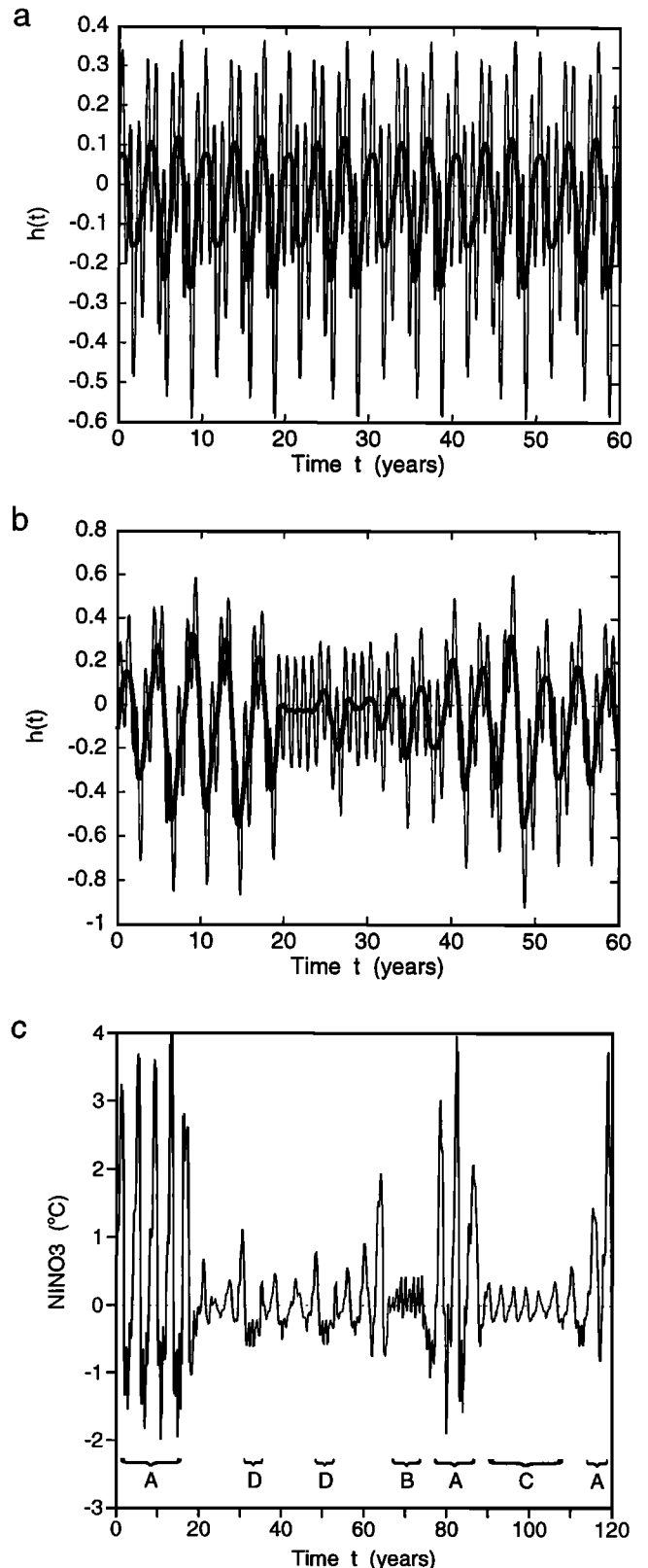


**Figure 1.** Time-series  $h(t)$  generated from Eq.1. The thick line portrays the smoothed time-series. (a) Quasiperiodic oscillations ( $D = 0$ ,  $\kappa = 1.4$ ). (b) Noise induced chaos ( $D = 0.2$ ,  $\kappa = 1.4$ ). (c) A segment of the CZ-model "standard run" in which the sea surface temperature (NINO3 index) exhibits regimes of periods: (A) 4-years; (B) 1-year; (C) 3-years. (D) Recurring unstable "cool event."

and Cane, 1987] suggest the existence of similar intermittencies between low-amplitude period-1 & -3 year cycles, and a more excited 4 year cycle in the SST anomaly. External noise forcing (or even internal "noise" in the form of inherent chaotic oscillations) has the capacity to perturb the trajectory of the SST anomaly, and allow it to wander randomly through these different dynamical regimes.

In order to examine Eq.1's intermittency effect in more detail, the probability of residing in a quiescent regime was plotted as a function of  $D$  (Fig.2a). For each time-series, we counted the total number of period-one cycles and determined their proportion, or "probability" of occurrence, in the entire time-series. (We also included in this count cycles that were deemed "close" or well within a defined distance from period-one, thus allowing for noise perturbed cycles. See [Lathrop, 1989] for complete details concerning detection of periodic cycles.) The resulting graph has a clear maximum at intermediate noise levels. An analysis of the probability of 3 and 4 year cycles in the time series yields a qualitatively similar graph which peaks at a different optimal noise intensity (Fig.2a). These results leads to the nonintuitive conclusion that increased noise in the system may lead to a maximum in signal coherence – an effect which is known as stochastic resonance (SR) [McNamara and Wiesenfeld, 1989; Wiesenfeld and Moss, 1995].

Threshold systems provide a simple and natural framework for understanding the SR mechanism [Gingl, et al., 1995; Wiesenfeld and Moss, 1995]. Consider, for example, the threshold effect displayed in the inset of Fig.2b, where the threshold is represented as a horizontal line. With no noise, the smoothed time-series  $h(t)$  is below the threshold (not displayed), and the ENSO signal goes undetected. However, in the presence of noise, the signal is sometimes reinforced and the threshold line is crossed (as displayed in Inset: top). On each occasion the resultant (signal+noise) crosses the threshold, an El Niño event is triggered and recorded as a pulse in another time-series (Inset: bottom).

As the noise-level  $D$  is increased, the threshold is crossed more frequently. Hints of the underlying ENSO signal emerge in the resulting pulse sequence. The signal-to-noise ratio (SNR) of the pulse sequence, evaluated at the ENSO frequency, initially tends to increase with  $D$ . On the other hand, too much noise ultimately drowns out the signal and the SNR deteriorates, so that the SNR has a characteristic maximum for an optimal noise intensity [Gingl, et al., 1995].

To examine this effect further in the context of Eq.1, successive model El Niño events were identified at each time,  $t_i$ , the smoothed time series  $h(t)$  (Fig.1a Legend) exceeded a predefined positive threshold level; a criteria that conforms with other definitions of El Niño [Cane, et al., 1986; Tziperman, et al., 1995]. (For the purposes of the following demonstration, the level was set so that in the absence of noise  $h(t)$  remained just below threshold.) Time-series of El Niño events,  $h^*(t)$ , were then constructed by setting  $h^*(t) = 1$ , if  $t = t_i$  and  $h^*(t) = 0$  otherwise (Fig.2b inset). A frequency spectrum analysis of the pulse train  $h^*(t)$  revealed two expected spikes at the dominant frequencies  $f_0$  and  $f_1$  and peaks at their harmonics. The SNR ratios were calculated for a range of noise levels at the ENSO frequency  $f_1$ . The SNR curve (Fig.2b) is "bell shaped" with a maximum at an optimal noise level, thus providing strong evidence for an SR effect [Gingl, et al., 1995]. The theoretical distribution of the SNR, as predicted by the SR theory,

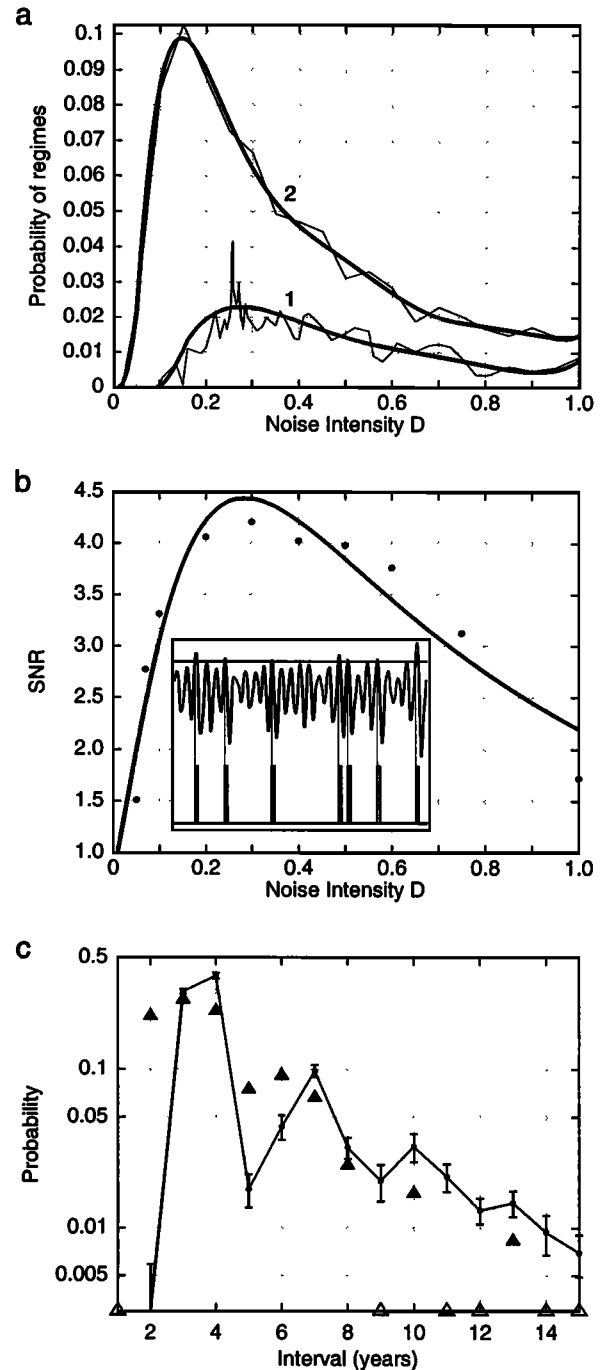


**Figure 2.** (a) Curve 1: Probability of the trajectory residing in a quiescent regime in model runs ( $\kappa = 1.4$ , 1,500 years) versus noise intensity  $D$ . Curve 2: probability of finding the trajectory on a 3 or 4 year cycle versus  $D$ . The thick lines are polynomial fits to the data.

(b) SNR ("•") of the pulse sequence  $h^*(t)$  versus  $D$ , as obtained from power spectrum analysis. The solid line is the least squares fit of the SNR predicted by Kramers formula. Inset: threshold mechanism (see text).

(c) Frequency histogram of interval in years between successive El Niño events represented by the black filled triangle symbol; the symbol " $\Delta$ " indicates a zero. Actual data taken from Quinn [1992] for the period 1492–1986. The thick curve is the average of 15 models runs ( $D = 0.3$ ) each of 5,000 years. Error bars portray one standard deviation.

is given by Kramers formula [McNamara and Wiesenfeld, 1989; Gingl, et al., 1995], and successfully fits the numerical results (Fig.2b). (A detailed explanation of the specific SR mechanisms, including the model's "internal" SR, may be found in [Neiman et al., 1997] and [Stone & Saparin ms.]).

The frequency distribution of the interval between El Niño events  $h^*(t)$  is plotted as a histogram in Fig. 2c. The histogram conforms with the SR theory [Wiesenfeld and Moss, 1995] which predicts a set of peaks that are: (a) located at multiples of the fundamental ENSO period, and (b) with an envelope (i.e., of the peaks) that decays exponentially. The same distribution is apparent in El Niño's historical record for the period 1492-1986 (data taken from [Quinn, 1992]), as shown in Fig.2c (see Legend).

## Discussion

SR implies that when noise levels are close to optimal, the effective ENSO 3-4 year signal manifests itself in the strongest possible way. Significant departures from the optimum lead to more erratic triggering of the El Niño, with very few events occurring sporadically when  $D$  is small (since the threshold is rarely crossed), and frequent but randomly timed events occurring for large  $D$ . Examination of the time-series makes clear that the most orderly and predictable behaviour in the evolution of the El Niño always occurs at intermediate noise levels, as guaranteed by the model's intrinsic SR.

There is no question that the environmental noise addressed in this study is a realistic phenomena operating on shorter time-scales than that taken into account in conventional ENSO models (but see [Lau, 1985; Jin, et al., 1996]). Apart from natural random background variation, the noise may for example be a product of short term local weather fluctuations including solar radiation anomalies, salinity anomalies, precipitation events, westerly wind bursts and other wind anomalies. All of the above factors lead to stochastic fluctuations in SST and thermocline depth, and may therefore be important driving forces behind the ENSO phenomenon. In view of these ever-present environmental fluctuations, the SR effects reported here need careful consideration for they indicate that should background levels of noise increase, the intensity, duration and frequency of El Niño could change significantly.

## References

- Cane, M. A., S. E. Zebiak, and S. C. Dolan, Experimental forecasts of El Niño, *Nature* 321, 827-832, 1986.
- Cane, M. A., S. E. Zebiak, and X. Yan, Model studies of the long term behavior of ENSO, *Proceedings of the 1992 Workshop on Decade to Century Time Scales of Natural Climate Variability* (in press).
- Chang, P., B. Wang, T. Li, and L. Ji, Interactions between the seasonal cycle and El Niño-Southern oscillation in an intermediate coupled ocean-atmosphere model, *J. Atmos. Sci.* 52, 2353-2371, 1995.
- Gingl, Z., L. B. Kiss, and F. Moss, Non-dynamical stochastic resonance: Theory and experiments with white and arbitrarily coloured noise, *Europhys. Lett* 29, 191-196, 1995.
- Graham, N. E., and W. B. White, The El Niño-Southern Oscillation as a natural oscillation of the tropical Pacific ocean-atmosphere system: Evidence from observation and models, *Science* 240, 1293-1302, 1988.
- Jin, F. F., D. Neelin, and M. Ghil, El Niño-Southern oscillation and the annual cycle: subharmonic frequency-locking and aperiodicity, *Physica D* 98, 442-465, 1996.
- Lathrop, D. P., and E. J. Kostelich, Characterization of an experimental strange attractor by periodic orbits, *Phys. Rev. A* 40, 4028-4031, 1989.
- Lau, K. M., Elements of a stochastic-dynamical theory of long-term variability of the El Niño-Southern oscillation. *J. Atmos. Sci.* 42, 1552-1558, 1985.
- McNamara, B., and K. Wiesenfeld, 1989 Theory of stochastic resonance. *Phys. Rev. A* 39, 4854-4869, 1989.
- Munnich, M., M. A. Cane, and S. E. Zebiak, A study of self-excited oscillations of the tropical ocean-atmosphere system. part II: Nonlinear cases, *J. Atmos. Sci.* 48, 1238-1248, 1991.
- Neiman, A., P. I. Saparin, and L. Stone, Coherence resonance and noisy precursors of bifurcations in nonlinear dynamical systems, *Phys. Rev. E* 270-273, 1997.
- Penland, C. and D. Sardeshmukh, The optimal growth of tropical sea surface temperature anomalies, *J. Climate* 8, 1999-2024, 1995.
- Quinn, W. H., A study of southern oscillation-related climatic activity for A.D. 622-1990 incorporating Nile river flood data, in *El Niño: Historical and Paleoclimatic Aspects of the Southern Oscillation*, edited by Diaz, H. F. and V. Markgraf, pp. 119-149, Cambridge University Press, Cambridge, 1992.
- Tziperman, E., L. Stone, M. A. Cane, and H. Jarosh, El Niño chaos: Overlapping of resonances between the seasonal cycle and the Pacific ocean-atmosphere oscillator, *Science* 264, 72-74, 1994.
- Tziperman, E., M. A. Cane, and S. E. Zebiak, Irregularity and locking to the seasonal cycle in an ENSO prediction model as explained by the quasi-periodicity route to chaos, *J. Atmos. Sci.* 52, 293-306, 1995.
- Wiesenfeld, K., and F. Moss, Stochastic resonance and the benefits of noise: from ice ages to crayfish and SQUIDS, *Nature* 373, 33-36, 1995.
- Zebiak, S. E., and M. A. Cane, A model El Niño-Southern Oscillation, *Mon. Wea. Rev.* 115, 2262-2278, 1987.

L. Stone, P. I. Saparin, A. Huppert, The Porter Super-Center for Ecological and Environmental Studies, Tel Aviv University, Ramat Aviv 69978, Tel Aviv, Israel, (e-mail: lewi@lanina.tau.ac.il; petr@agnld.uni-potsdam.de; amit@lanina.tau.ac.il)

C. Price, Department of Geophysics and Planetary Sciences, Tel Aviv University, Ramat Aviv, 69978, Tel Aviv, Israel, (e-mail: cprice@flash.tau.ac.il)

(Received May 16, 1997; revised September 10, 1997; accepted November 6, 1997.)